

# Faraday Discussions

Accepted Manuscript



This manuscript will be presented and discussed at a forthcoming Faraday Discussion meeting. All delegates can contribute to the discussion which will be included in the final volume.

**Register now to attend!** Full details of all upcoming meetings: <http://rsc.li/fd-upcoming-meetings>



This is an *Accepted Manuscript*, which has been through the Royal Society of Chemistry peer review process and has been accepted for publication.

*Accepted Manuscripts* are published online shortly after acceptance, before technical editing, formatting and proof reading. Using this free service, authors can make their results available to the community, in citable form, before we publish the edited article. We will replace this *Accepted Manuscript* with the edited and formatted *Advance Article* as soon as it is available.

You can find more information about *Accepted Manuscripts* in the [Information for Authors](#).

Please note that technical editing may introduce minor changes to the text and/or graphics, which may alter content. The journal's standard [Terms & Conditions](#) and the [Ethical guidelines](#) still apply. In no event shall the Royal Society of Chemistry be held responsible for any errors or omissions in this *Accepted Manuscript* or any consequences arising from the use of any information it contains.

**Vibrational Dynamics of the CO Stretching of 9-Fluorenone Studied by Visible-pump  
and Infrared-probe Spectroscopy**

**Yuki Fukui, Kaoru Ohta, and Keisuke Tominaga**

Department of Chemistry, Graduate School of Science, Kobe University,

Molecular Photoscience Research Center, Kobe University,

Nada, Kobe, 657-8501 Japan

e-mail address: tominaga@kobe-u.ac.jp

**Abstract**

We studied effects of hydrogen bond on the vibrational structures and the vibrational dynamics of the CO stretching mode of 9-fluorenone (FL) in the electronically excited state in aprotic and protic solvents by sub-picosecond visible-pump and IR-probe spectroscopy. The transient IR spectrum of the CO stretching band in methanol- $d_4$  has bands at 1529.9  $\text{cm}^{-1}$  and 1543.4  $\text{cm}^{-1}$ . We assigned the two bands at 1529.9  $\text{cm}^{-1}$  and 1543.4  $\text{cm}^{-1}$  to a FL complex with solvent and free FL, respectively. In the aprotic solvents, the CO stretching bands show blue-shifts in time. This shift is due to vibrational cooling, which is derived from anharmonic couplings by some low-frequency modes. Interestingly, a red-shift is observed at later delay time for the band at 1529.9  $\text{cm}^{-1}$  in methanol- $d_4$ . A possible mechanism of this spectral shift is related to the hydrogen bond dynamics between the solute and solvent.

## Introduction

In a solution, a solute molecule relaxes to the most stable state of the electronically excited state ( $S_1$ ) after the electronic excitation to the Franck-Condon state through various relaxation processes. These processes are, for example, a vibrational energy relaxation, a cooling process of the locally heated environment around the solute, and solvation dynamics [1-8]. They influence chemical reactions initiated by the electronic excitation. In a protic solvent, a solute molecule forms intermolecular hydrogen bonds with solvents if the solute has hydrogen bonding sites such as a carbonyl group. The hydrogen bonds influence various properties of solute such as its electronic states, the relaxation processes, and so on.

9-Fluorenone (FL) has a carbonyl group which can form hydrogen bonds, and spectroscopic studies [9-14] as well as theoretical calculations [15] have been reported on the nature of the excited state of FL. The vibrational dynamics of FL in alcohol solutions were previously reported in the electronically ground state [12] and the excited state [10,13,14]. By sub-picosecond UV-pump infrared (IR)-probe spectroscopy we observed transient IR absorption spectra of FL in acetonitrile- $d_3$  and methanol- $d_4$  [13]. From comparison with theoretical calculation of the vibrational structure in the  $S_1$  state [15], we assigned vibrational bands observed in the transient spectra. In this study, by

sub-picosecond visible-pump and IR-probe spectroscopy we study effects of hydrogen bond on the vibrational structures and the vibrational dynamics of the CO stretching mode of the excited state FL in various solvents including a protic solvent.

### **Experimental**

Details of the experimental setup are as follows. The pump pulse was generated by frequency doubling of the output of a Ti:sapphire regenerative amplifier. The tunable IR pulse was generated by difference frequency mixing of the signal and idler outputs of the optical parametric amplifier. The probe and reference pulses were obtained using the reflection of a CaF<sub>2</sub> wedged window. The probe and reference pulses were dispersed by a monochromator and the absorption changes were measured with a 32-channel MCT (HgCdTe) array detector. The experiments were conducted using 100- $\mu$ m-thick liquid samples in a rotating cell. The concentrations of FL were 45 mM for all the solutions.

FL was purchased from Sigma-Aldrich and recrystallized from ethanol once before use. Aprotic solvents (cyclohexane, acetonitrile-*d*<sub>3</sub>, tetrahydrofuran (THF), and dimethyl sulfoxide (DMSO) from Sigma-Aldrich) and a protic solvent (methanol-*d*<sub>4</sub> from Merck) were used as received.

We obtained optimized geometries and frequencies of normal mode coordinates of the electronically ground state of FL in gas phase by performing density functional theory (DFT) calculations with a basis set of 6-31++G(d, p) using the B3LYP function with Gaussian 03. Calculations for the hydrogen-bonded complex were also conducted. For the  $S_1$  state time-dependent (TD) DFT calculation was performed with the B3LYP functional and the 6-31G(d, p) basis set. The solvent effect was taken into account by Self-Consistent Reaction Field theory with Polarizable Continuum Model with certain dielectric constant of solvent.

### Results and Discussion

Figure 1 shows steady-state IR absorption spectra of FL in acetonitrile- $d_3$  and methanol- $d_4$ . In aprotic solvents such as acetonitrile- $d_3$  a sharp, single band due to the CO stretching mode of FL is observed, which is reproduced well with a single Lorentzian function. As for protic solvents like methanol- $d_4$ , three Lorentzian functions are required to simulate the CO stretching band. From comparison with normal modes obtained by the DFT calculations Hirai and coworkers showed that the highest wavenumber band (band *a* in Figure 1) is assigned as the CO stretching band of FL which does not form hydrogen bond with solvent (abbreviated as [FL] hereafter), the next highest band (band *b*) as the band of

FL which is hydrogen-bonded with one alcohol molecule ([FL:ROH]), and the lowest wavenumber band (band *c*) as the band of FL with two alcohol molecules ([FL:(ROH)<sub>2</sub>]) [12]. In this work we also used Gaussian functions to fit the spectrum, and it is found that the Lorentzian function gives better spectral simulation results. Of course, it is possible to simulate the spectra with Gaussian functions, and the final conclusion will be different from that obtained by Lorentzian functions.

In Table I we summarize the peak wavenumbers of the CO stretching band of FL in various solvents. It is seen that in more polar solvents the peak wavenumber shifts toward the lower-frequency side. This is because the vibrational excited state is more stabilized energetically in polar solvents. Levinson et al. explained solvatochromism of the CN stretching band of benzonitrile and 4-aminobenzonitrile in terms of the Onsager factor ( $F_{onsager}$ ), a parameter indicating polarity of solvent [16]. In the model a solute is assumed to be a spherical cavity in a continuum with dielectric constant  $\epsilon$  and refractive index  $n$ . The Onsager reaction field can be expressed as,

$$F_{onsager} = \frac{2(\epsilon - 1)(n^2 + 2)}{3(2\epsilon + n^2)}. \quad (1)$$

In Figure 2 the peak frequencies of the CO stretching band of FL in aprotic solvents and free FL in methanol- $d_4$  (band  $a$  in Figure 1) is plotted as a function of  $F_{\text{onsager}}$ . A good correlation is observed in the relation between the peak frequency and  $F_{\text{onsager}}$ .

Figure 3 shows time evolutions of the transient IR absorption spectra of FL in the electronically excited state in acetonitrile- $d_3$  and methanol- $d_4$ . The observed wavenumber region is 1492 – 1576  $\text{cm}^{-1}$ . We first discuss the results for the acetonitrile- $d_3$  case. We show a transient spectrum at 48 ps together with spectral simulation using three Lorentzian functions in Figure 4. These three bands are named as bands  $a$ ,  $a'$ , and  $d$  from the higher wavenumber side. In Table II the peak frequencies of the bands in several aprotic solvents are summarized. The band position of the band  $d$  depends on the solvent, and in cyclohexane and THF band  $d$  is not observed; it is probably located below 1492  $\text{cm}^{-1}$ . By nanosecond time-resolved IR spectroscopy Tanaka et al. found that the CO stretching band of FL in the  $S_1$  state is located at 1544  $\text{cm}^{-1}$  in acetonitrile- $d_3$  [10]. They observed an isotope shift caused by substitution of  $^{16}\text{O}$  to  $^{18}\text{O}$  in the carbonyl group of FL. Therefore, the band  $a$  is assigned as the CO stretching mode of FL in the  $S_1$  state. Furthermore, the band  $d$  is located at 1495.7  $\text{cm}^{-1}$ , which corresponds to a band at 1496  $\text{cm}^{-1}$  Tanaka et al. observed previously. From the TD-DFT calculation we obtain the normal modes and vibrational frequencies in the  $S_1$  state in acetonitrile. The CO stretching



band is predicted to be at  $1644.5\text{ cm}^{-1}$ . Other bands in this wavenumber region are a band at  $1637.4\text{ cm}^{-1}$  in which the CO stretching mode and a fluorene ring mode are coupled, and a band at  $1604.7\text{ cm}^{-1}$  corresponding to the vibrational mode localized in the fluorene ring. It is suggested that these modes correspond to the experimentally observed bands at  $1533.2\text{ cm}^{-1}$  (band *a'*) and  $1495.7\text{ cm}^{-1}$  (band *d*) in acetonitrile- $d_3$ , respectively, although the agreement between the calculation and experiment is not perfect. We summarize the computed frequencies in Table III, and normal mode pictures are shown in Figure 5.

In Figure 6 time evolution of the peak wavenumber of the band *a* is shown in acetonitrile- $d_3$ . The band shows a blue-shift as a function of delay time. The time dependence is simulated well in terms of a bi-exponential function with time constants of  $1.1\pm 0.2\text{ ps}$  and  $10.5\pm 0.4\text{ ps}$ . The other two bands, bands *a'* and *d*, also show similar blue-shifts. This blue-shift is suggested to be due to vibrational cooling [17]. The high-frequency intramolecular modes of FL are anharmonically coupled to the low-frequency bath modes. After photoexcitation, the vibrational energy relaxation takes place from the Franck-Condon state to the vibrational ground state in the  $S_1$  state. The solute molecule in the excited state is locally heated because of excess energy which is dissipated into the intramolecular degrees of freedom and local environment surrounding the solute. The vibrationally hot  $S_1$  state is cooled down due to thermal diffusion, which

causes a blue-shift of the vibrational band because of the anharmonic coupling with the bath modes. This vibrational cooling has been observed in other solution systems, which show a picosecond time scale for this process [17,18].

In the right panel of Figure 3 we display time evolution of the transient IR absorption spectra of FL in the electronically excited state in methanol- $d_4$ . The band at  $1544.7\text{ cm}^{-1}$  is assigned as the CO stretching band of free FL from similarity of the band shape and peak wavenumber to the band *a* in the aprotic solvents. A band at  $1532.2\text{ cm}^{-1}$  is not observed in aprotic solvents. This band becomes prominent as the delay time increases. In order to make assignment of this band we measured transient vibrational spectra in binary mixtures of dimethyl sulfoxide (DMSO) and methanol- $d_4$ . The transient spectra at delay time of 48 ps are shown in Figure 7 with different concentrations of methanol- $d_4$ . In pure DMSO the transient spectrum is similar to that in acetonitrile- $d_3$ . With increasing the concentration of methanol- $d_4$  this band (named as band *b*) becomes clear as seen from the figure. The band *b* is characteristic to protic solvents, therefore, we conclude that the band *b* is the CO stretching mode of FL which is hydrogen-bonded with methanol- $d_4$ , [FL:CD<sub>3</sub>OD]. It should be noted that at  $t = 1.0\text{ ps}$  in Figure 3 the band *b* in methanol- $d_4$  is not clearly observed, and the spectral shape looks like that in acetonitrile- $d_3$ . This fact suggests that just after the photoexcitation FL which forms a hydrogen bond with the

solvent in the  $S_0$  state experiences hydrogen bond breakage. With increase of the delay time, hydrogen bonds are formed in the excited  $S_1$  state again. At  $t = 3.0$  ps a shoulder peak at around  $1530\text{ cm}^{-1}$  is already observed, suggesting that the hydrogen-bond formation takes place within this time scale.

Since the band  $b$  is located in the lower wavenumber side than the band  $a$ , the CO stretching band of FL in the  $S_1$  state is red-shifted by formation of hydrogen bond with solvent, similarly to the case of the  $S_0$  state. This trend is also reproduced by the TD-DFT calculation. In Table III the calculation results for the methanol solvent are also summarized. When the carbonyl group is hydrogen-bonded with one methanol solvent, the vibrational wavenumber is shifted to  $1624.5\text{ cm}^{-1}$ , about  $20\text{ cm}^{-1}$  lower side than the free FL case.

For the  $S_0$  state in methanol- $d_4$ , a hydrogen-bonded complex  $[\text{FL}:(\text{CD}_3\text{OD})_2]$  is observed in the IR absorption spectrum. In the  $S_1$  state, the band  $d$  was once assigned as the CO stretching mode of  $[\text{FL}:(\text{CD}_3\text{OD})_2]$  by sub-picosecond visible-pump IR-probe spectroscopy [14]. However, we observe the band  $d$  even in the aprotic solvents such as DMSO. Therefore, we conclude that the band  $b$  is not due to  $[\text{FL}:(\text{CD}_3\text{OD})_2]$ , but due to free FL. Since the TD-DFT calculation predicts that the CO stretching mode is more red-shifted when FL forms more hydrogen bonds with solvents, it is deduced that the CO

stretching band of  $[\text{FL}:(\text{CD}_3\text{OD})_2]$ , if it exists, will be located in the lower frequency side than the bands  $a$  or  $b$ . However, we do not observe such a band in that frequency region beside the band  $d$ . Thus, it is suggested that hydrogen-bonded complex  $[\text{FL}:(\text{CD}_3\text{OD})_2]$  does not exist in the  $S_1$  state, probably due to a weaker hydrogen bond between FL in the  $S_1$  state and the solvent molecule than that in the  $S_0$  state.

In aprotic solvents we observe the band  $a'$ , which is formed by mixing of the CO stretching mode and fluorene ring vibrational mode. Similarly, in protic solvents it is natural to assume that this mixed mode exists for free FL. Actually, from the TD-DFT calculation it is predicted that the band  $a'$  is located at  $1637.4\text{ cm}^{-1}$  and the fluorene ring mode is at  $1640.7\text{ cm}^{-1}$  for free FL in methanol. Furthermore, a shoulder band is observed at  $1550.2\text{ cm}^{-1}$  in methanol, which is not observed in aprotic solvents and named as band  $c$ . The TD-DFT calculation shows that the mixed mode (band  $a'$ ) is blue-shifted from  $1637.4\text{ cm}^{-1}$  to  $1644.3\text{ cm}^{-1}$  by formation of hydrogen-bond with solvent, in contrast to the case of the CO stretching band. In our previous work we assigned the bands  $a$  and  $b$  as the CO stretching modes of free FL and the complex  $[\text{FL}:\text{CD}_3\text{OD}]$ , respectively, which is opposite to the present conclusion, from comparison with the TD-DFT calculation with B3LYP/TZVP level [15]. They concluded that the bands at  $1592\text{ cm}^{-1}$  and  $1595\text{ cm}^{-1}$  are the CO stretching modes of free FL and the complex  $[\text{FL}:\text{CD}_3\text{OD}]$ , respectively. We

performed the TD-DFT calculation with the same basis set for free FL and the hydrogen-bonded complex and obtained similar results to those in frequency. However, from the normal mode picture, it is found that the bands at  $1590\text{ cm}^{-1}$  and  $1592\text{ cm}^{-1}$  are not the CO stretching modes, but the fluorene ring modes of free FL and the hydrogen-bonded complex, respectively. The CO stretching bands of free FL and the complex are located at  $1626\text{ cm}^{-1}$  and  $1619\text{ cm}^{-1}$ , respectively. They might confuse the fluorene ring mode with the CO stretching mode.

To summarize, there are five bands to simulate the transient spectra of FL in protic solvent such as methanol; three of them (bands *a*, *a'*, and *d*) are observed in aprotic solvents also, and the rest of two (bands *b* and *c*) are observed only in protic solvents. To simulate the spectra with five Lorentzian functions we make the following assumption. It is expected that the wavenumbers of the bands *a'* and *b* are very close each other, so that it is difficult to separate them in the spectral simulation. We assume that the wavenumber difference and the relative intensities between the bands *a* and *a'* for the methanol solvent case are the same as those for the acetonitrile case since the polarities of the two solvents are similar. We first obtain time evolutions of the wavenumber difference and the relative intensities between the bands *a* and *a'* for the acetonitrile case from the spectral analysis and use these results for the analysis of the methanol case. The result of the spectral

analysis using five Lorentzian functions is shown in Figure 4, and the peak wavenumbers of the five bands are summarized in Table IV.

In Figure 6 the time evolutions of the peak wavenumbers of the bands *a* and *b* are displayed. The band *a* shows a blue-shift, which is reproduced well in terms of a single exponential function with a time constant of  $10.0 \pm 0.2$  ps. Similarly to the aprotic solvent cases, this blue-shift is due to vibrational cooling. Interestingly, the band *b* first shows a blue-shift which is followed by a red-shift. The time dependence is simulated by a bi-exponential function with time constants of  $3.9 \pm 1.4$  ps (blue-shift) and  $11.1 \pm 6.9$  ps (red-shift). It seems two different dynamics cause the vibrational frequency shift in an opposite manner. The blue-shift is probably due to vibrational cooling. However, it should be noted that the hydrogen bond formation also occurs in this early time scale ( $t < 3$  ps) as mentioned previously. On the other hand, the red-shift may be related to the hydrogen bond between the solute and solvent since only the hydrogen-bonded complex shows this red-shift. Possible dynamics for this is structural rearrangement of the hydrogen-bonded complex, and there are two conceivable mechanisms which cause this rearrangement; one is that the hydrogen-bonded complex relaxes to most stable state by cooling in the surrounding environment around the complex. The other is that by the polarization relaxation in the solvent (solvation dynamics) reorganization of the solvent molecules

takes place, which causes the rearrangement of the structure of the hydrogen-bonded complex. At present it is difficult to distinguish which mechanism, cooling or solvation dynamics, is more dominant for this red-shift.

In Figure 8 we plot the peak wavenumbers of the band *a* as a function of solvent polarity  $F_{\text{onsager}}$ . In the  $S_0$  state we observe good correlation between the peak wavenumber and  $F_{\text{onsager}}$ ; the peak frequency of the CO stretching mode shifts to lower frequency side as a function of the solvent polarity. However, in the  $S_1$  state such a good correlation is not observed in Figure 7. This is probably because that the electronic structure of the  $S_1$  state depends on the solvent polarity so that the vibrational structure of the  $S_1$  state is also influenced by the solvent. It is well known that the  $n\pi^*$  and  $\pi\pi^*$  states are mixed in the electronically excited state of FL and the degree of the mixing depends on the solvent polarity.

## Conclusion

The transient vibrational spectra of FL were obtained in both aprotic and protic solvents by sub-picosecond visible-pump and IR-probe spectroscopy. The transient IR spectrum of the CO stretching band in methanol- $d_4$  has peaks at  $1529.9\text{ cm}^{-1}$  and  $1543.4\text{ cm}^{-1}$ , which are assigned as bands of hydrogen-bonded complex with solvents and free FL,

respectively. In the aprotic solvents, the CO stretching bands show blue-shifts in time, which is due to vibrational cooling. The free FL in methanol- $d_4$  also shows the same blue-shift. However, red-shift is observed at later time for the band at  $1529.9\text{ cm}^{-1}$  in methanol- $d_4$ . Hydrogen bond dynamics between FL and solvent molecules may be related to this red-shift.

### **Acknowledgment**

We thank Dr. Masahiro Higashi of University of the Ryukyus and Prof. Shinji Saito of Institute for Molecular Science for helpful discussion, especially on theoretical calculation. Theoretical calculations were performed using Research Center for Computational Sciences, Okazaki, Japan. The authors thank Prof. Dipak K. Palit of Bhabha Atomic Research Centre for valuable discussion.



**References**

1. H. Hamaguchi, and T. L. Gustafson, *Ann. Rev. Phys. Chem.* **45**, 593–622 (1994).
2. P. Hamm and W. Zinth, *J. Phys. Chem.* **99**, 13537–13544 (1995)
3. C. Chudoba, E. T. J. Nibbering, and T. Elsaesser, *J. Phys. Chem. A* **103**, 5625–5628 (1999).
4. E. T. J. Nibbering, F. Tschirschwitz, C. Chudoba, and T. Elsaesser, *J. Phys. Chem. A* **104**, 4236–4246 (2000).
5. J. B. Asbury, Y. Wang, and T. Lian, *Bull. Chem. Soc. Jpn.* **75**, 973–983 (2002).
6. W.-M. Kwok, M. W. George, D. C. Grills, C. Ma, P. Matousek, A. W. Parker, D. Phillips, W. T. Toner, and M. Towrie, *Angew. Chem. Int. Ed.* **42**, 1826–1830 (2003).
7. E. T. J. Nibbering, H. Fidder and E. Pines, *Ann. Rev. Phys. Chem.* **56**, 337–367 (2005).
8. P. Kukura, D. W. McCamant, and R. A. Mathies, *Ann. Rev. Phys. Chem.* **58**, 461–488 (2007).
9. K. Yoshihara and D. R. Kearns, *J. Chem. Phys.* **45**, 1991–1999 (1966).
10. S. Tanaka, C. Kato, K. Horie, and H. Hamaguchi, *Chem. Phys. Lett.* **381**, 385–391 (2003).

11. V. Samant, A. K. Singh, G. Ramakrishna, H. N. Ghosh, T. K. Ghanty, and D. K. Palit, *J. Phys. Chem. A* **109**, 8693–8704 (2005).
12. S. Hirai, M. Banno, K. Ohta, D. K. Palit, and K. Tominaga, *Chem. Phys. Lett.* **450**, 44–48 (2007).
13. S. Hirai, M. Banno, K. Ohta, D. K. Palit, and K. Tominaga, *Chem. Lett.* **39**, 932–934 (2010).
14. H. N. Ghosh, K. Adamczyk, S. Verma, J. Dreyer, and E. T. J. Nibbering, *Chem. Eur. J.* **18**, 4930–4937 (2012).
15. G.-J. Zhao and K.-L. Han, *J. Phys. Chem. A* **111**, 9218–9223 (2007).
16. N. M. Levinson, S. D. Fried, and S. G. Boxer, *J. Phys. Chem. B* **116**, 10470–10476 (2012).
17. P. Hamm, S. M. Ohline, and W. Zinth, *J. Chem. Phys.* **106**, 519–529 (1997).
18. K. Iwata and H. Hamaguchi, *J. Phys. Chem. A* **101**, 632–637 (1997).

**Table I. Peak wavenumbers of the vibrational bands in the IR absorption spectrum of FL in various solvents.**

aprotic solvents	Peak wavenumber (cm <sup>-1</sup> )		
cyclohexane	1725.3±0.1		
acetonitrile- <i>d</i> <sub>3</sub>	1717.9±0.1		
Tetrahydrofurane	1719.7±0.1		
Dimethyl sulfoxide	1714.3±0.1		
protic solvent	band <i>a</i>	band <i>b</i>	band <i>c</i>
methanol- <i>d</i> <sub>4</sub>	1720.9±0.1	1712.5±0.1	1702.6±0.5

**Table II. Peak wavenumbers of the vibrational bands in the transient IR absorption spectrum of FL in aprotic solvents.**

	band $a/\text{cm}^{-1}$	band $a'/\text{cm}^{-1}$	band $d/\text{cm}^{-1}$
cyclohexane	1540.0 $\pm$ 0.5	1533.7 $\pm$ 2.9	-
acetonitrile- $d_3$	1542.4 $\pm$ 0.2	1533.2 $\pm$ 0.8	1495.7 $\pm$ 0.5
Tetrahydrofurane	1539.1 $\pm$ 0.3	1529.8 $\pm$ 2.2	-
Dimethyl sulfoxide	1539.7 $\pm$ 0.4	1531.8 $\pm$ 1.3	1494.1 $\pm$ 0.8

**Table III. Computed wavenumbers of FL in the  $S_1$  state by TD-DFT.<sup>a)</sup>**

SCRF	$\epsilon$	number of hydrogen bonds	wavenumbers/cm <sup>-1</sup>		
			CO stretching mode	CO stretching and fluorene ring mode	fluorene ring mode
acetonitrile	36.64		1644.5	1637.4	1604.7
methanol	24.55	0	1644.6	1637.4	1604.7
		1	1624.5	1644.3	1605.3
		2	1611.5	1645.2	1604.8

a) Normal mode pictures are shown in Figure 5.

**Table IV. Peak wavenumbers of the vibrational bands in the transient IR absorption spectrum of FL in methanol- $d_4$ .<sup>a)</sup>**

	band <i>c</i>	band <i>a</i>	band <i>a'</i>	band <i>b</i>	band <i>d</i>
Peak wavenumber (cm <sup>-1</sup> )	1550.0±0.7	1543.4±0.3	1534.2±0.3	1529.9±0.3	1501.8±0.3

**Figure captions**

**Figure 1.** FTIR spectra of FL in acetonitrile- $d_3$  (upper) and methanol- $d_4$  (lower).

Results of the spectral simulation are also shown.

**Figure 2.** Peak wavenumbers of the free FL (band  $a$ ) in the  $S_0$  state as a function of solvent polarity.

**Figure 3.** Time evolution of transient IR spectra of FL in acetonitrile- $d_3$  (left) and methanol- $d_4$  (right).

**Figure 4.** Transient IR spectra of FL in acetonitrile- $d_3$  (upper) and methanol- $d_4$  (down) at delay time of 48 ps. The results of the spectral simulation are shown.

**Figure 5.** Computed normal modes of FL in the  $S_1$  state by TD-DFT. CO stretching mode (left), mixed mode of CO stretching mode and fluorene ring mode (middle), fluorene ring mode (right).

**Figure 6.** Time evolutions of the peak wavenumbers of the transient IR spectra of FL. Band  $a$  in acetonitrile- $d_3$  (left), band  $a$  in methanol- $d_4$  (middle), and band  $b$  in methanol- $d_4$  (right).

**Figure 7.** Transient IR spectra of FL in a binary solvent of methanol- $d_4$  and DMSO at delay time of 48 ps. The concentrations in molar ratio are indicated in the figure.

**Figure 8.** Peak wavenumbers of the free FL (band  $a$ ) in the  $S_1$  state as a function of solvent polarity.



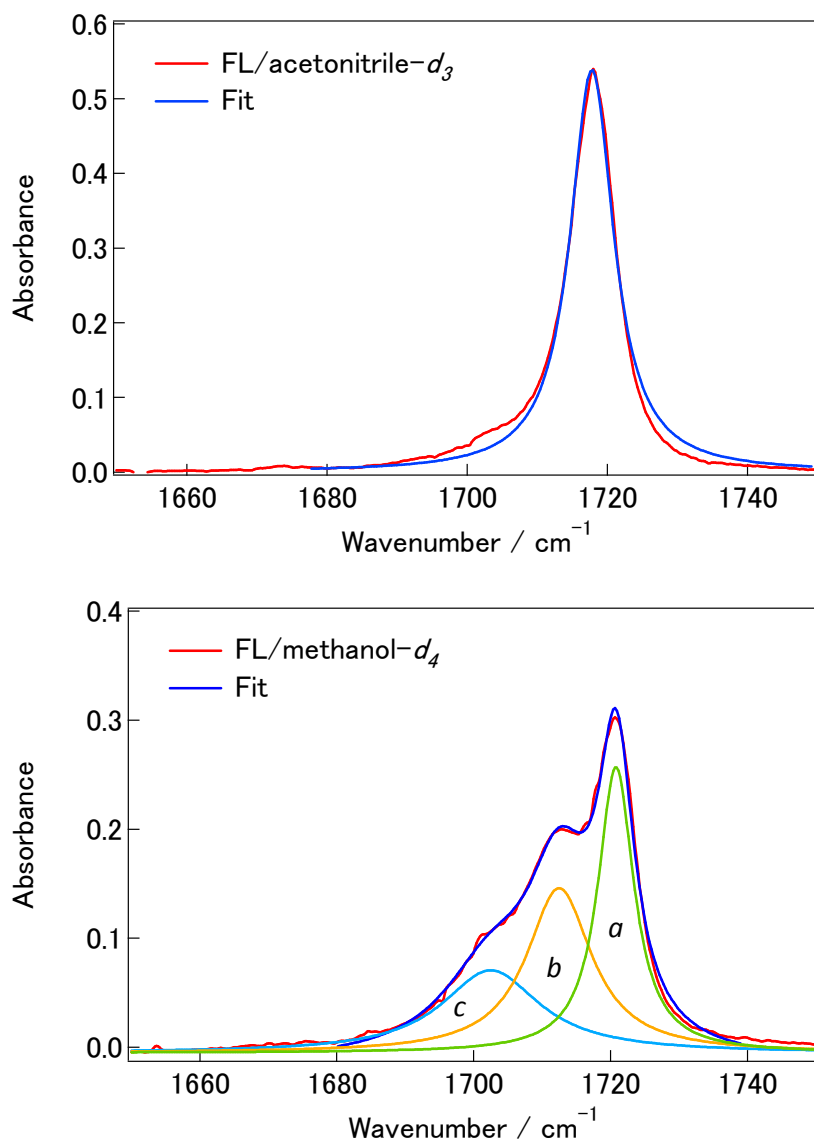


Figure 1.

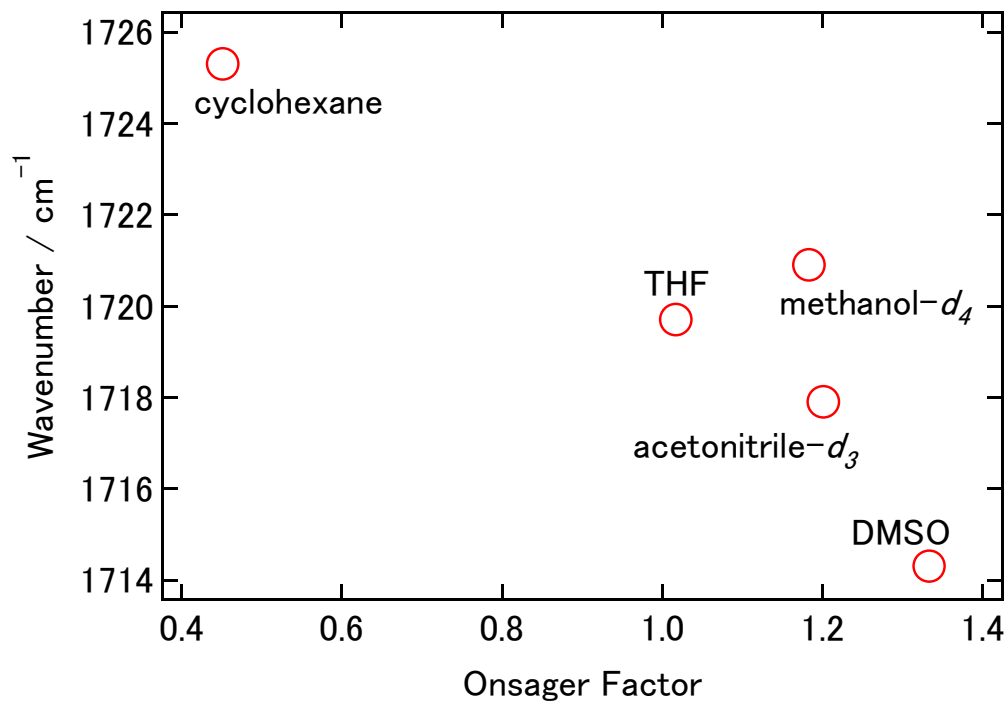


Figure 2.

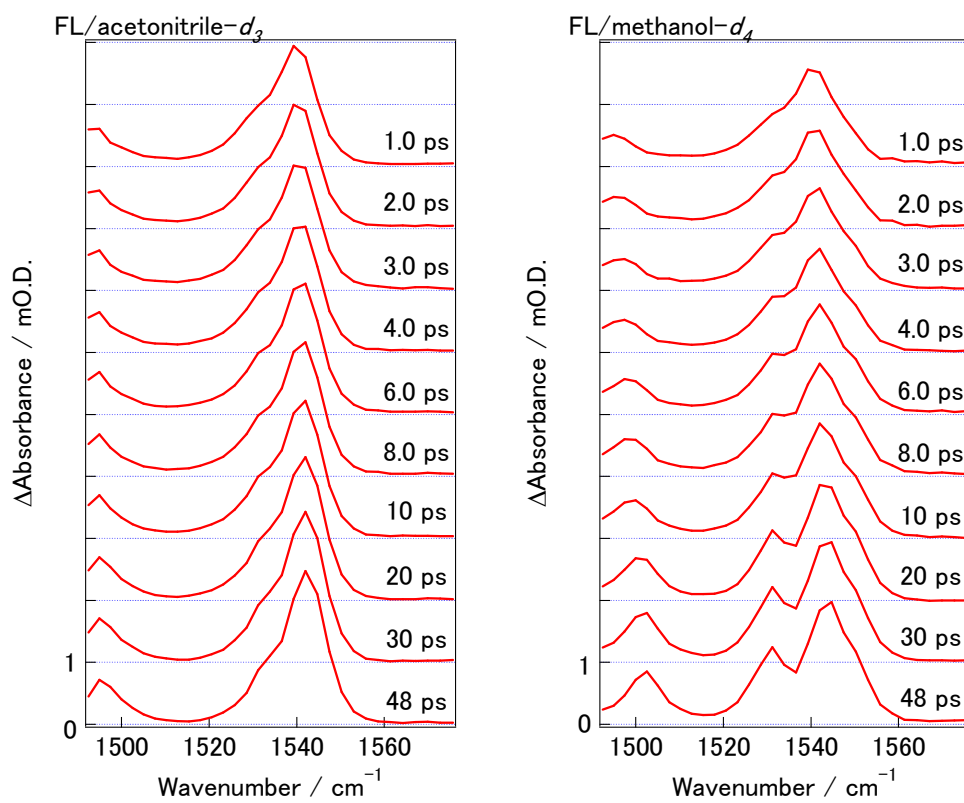


Figure 3.

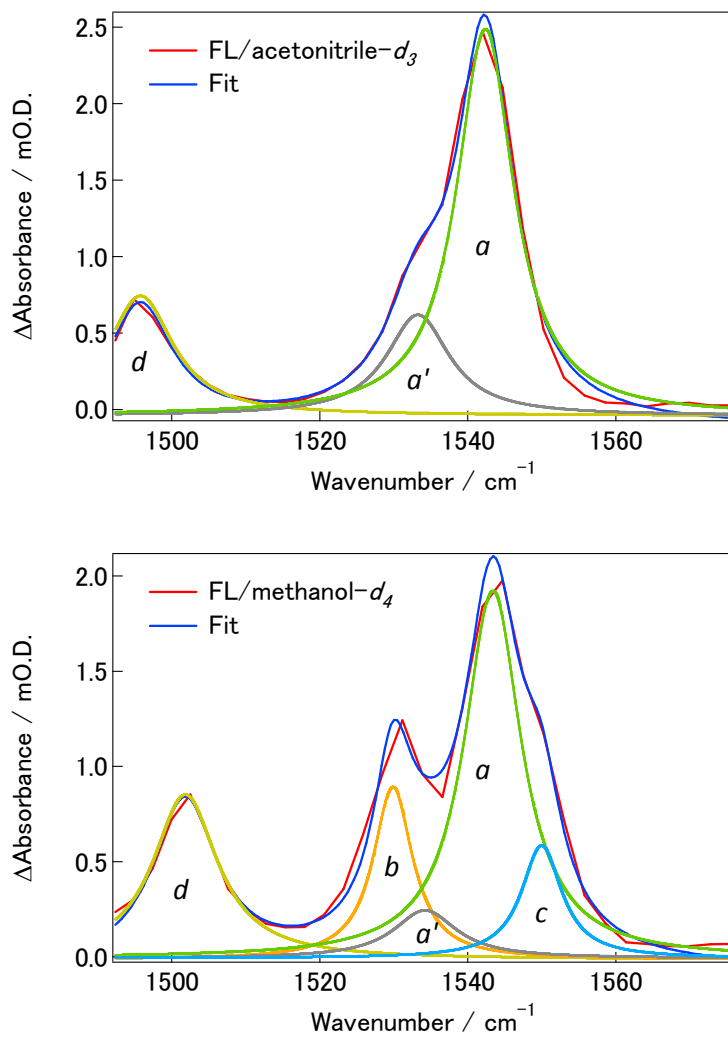
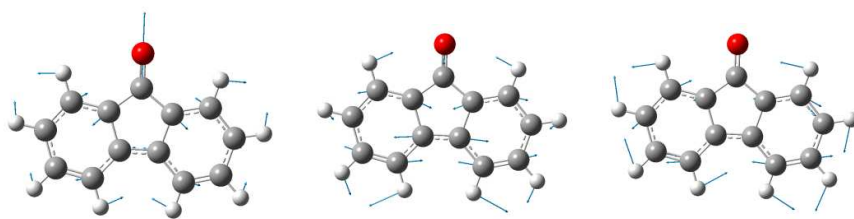


Figure 4.



**Figure 5.**

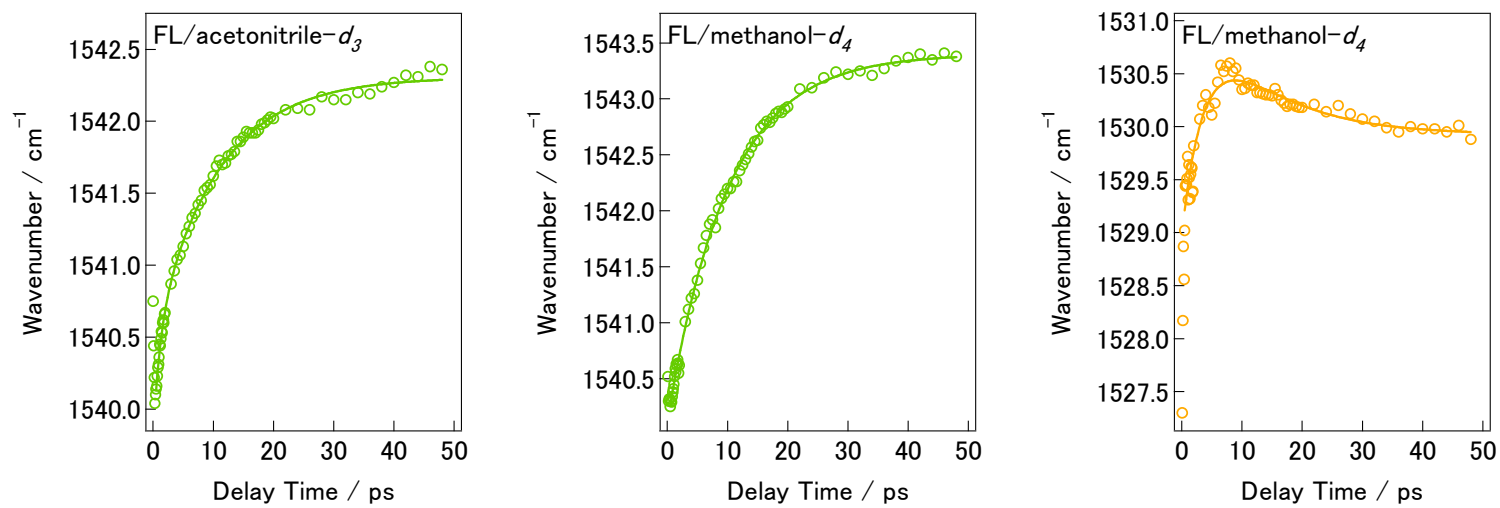


Figure 6.

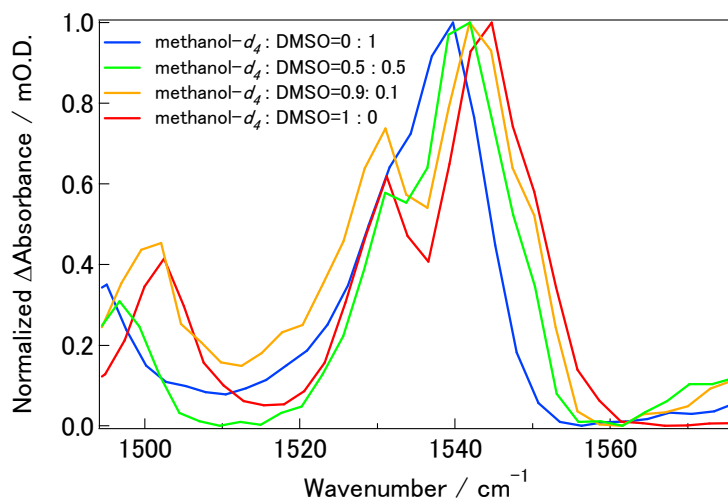


Figure 7.

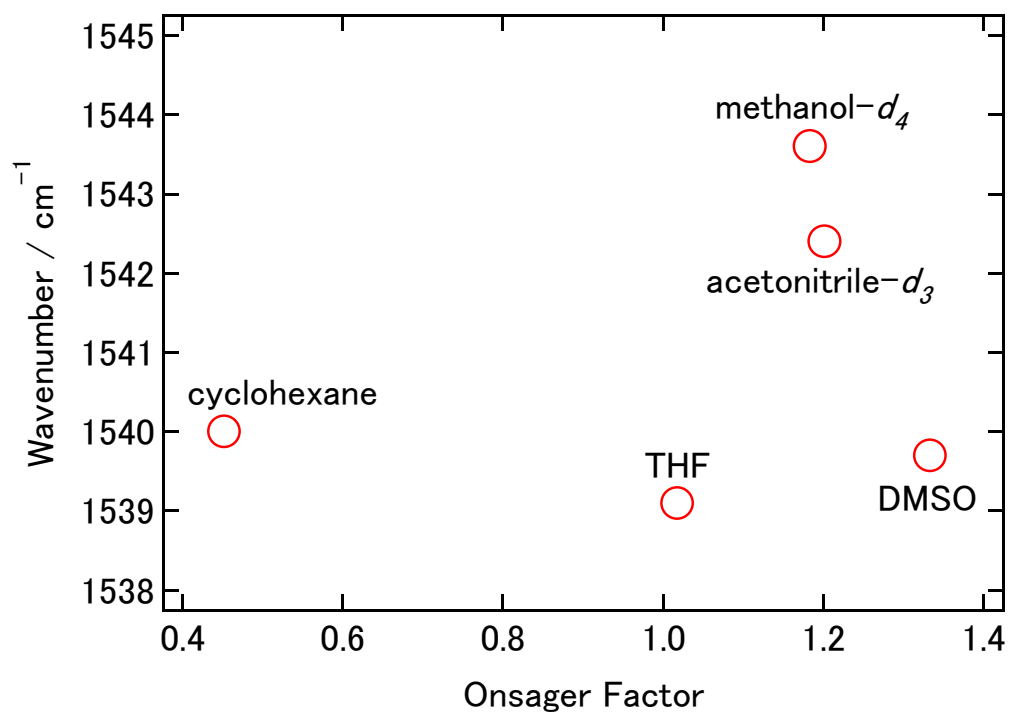


Figure 8.